Inorganic Chemistry

Article

pubs.acs.org/IC

Violating the Isolated Pentagon Rule (IPR): Endohedral Non-IPR C_{98} Cages of $Gd_2@C_{98}$

Xiang Zhao,*[,†] Wei-Yin Gao,[†] Tao Yang,[†] Jia-Jia Zheng,[†] Le-Sheng Li,[†] Ling He,[†] Rui-Jun Cao,[†] and Shigeru Nagase*[,‡]

[†]Institute for Chemical Physics and Department of Chemistry, Xi'an Jiaotong University, Xi'an 710049, China

[‡]Department of Theoretical and Computational Molecular Science, Institute for Molecular Science, Okazaki, 444-8585, Japan

Supporting Information

ABSTRACT: The geometric, electronic structure, and thermodynamic stability of large gadolinium-containing endohedral metallofullerenes, $Gd_2@C_{98}$, have been systematically investigated by comprehensive density functional theory calculations combined with statistical mechanics treatments. The $Gd_2@C_2(230924)$-C_{98} structure, which satisfies the isolated-pentagon rule (IPR), is determined to possess the lowest energy followed with some stable non-IPR isomers. In order to clarify the relative stabilities at elevated temperatures, entropy contributions are taken into account on the basis of the Gibbs energy at the B3LYP level for the first time. Interestingly, a novel non-IPR $Gd_2@C_1(168785)$-C_{98} isomer which has one pair of pentagon adjacency is more thermodynamically stable than the lowest energy IPR species within a wide temperature interval related to fullerene formation. Therefore, the $Gd_2@C_1(168785)$-C_{98} is predicted to be the most proper isomer obtained experimentally, which is the largest non-IPR carbon cage found so far. Our findings demonstrate that interaction between metals and carbon cages could stabilize the fused pentagons effectively, and thus, the non-IPR isomers should not be ignored in some cases of endohedral metallofullerenes. The IR features of $Gd_2@C_{98}$ are simulated to assist its future experimental characterization.

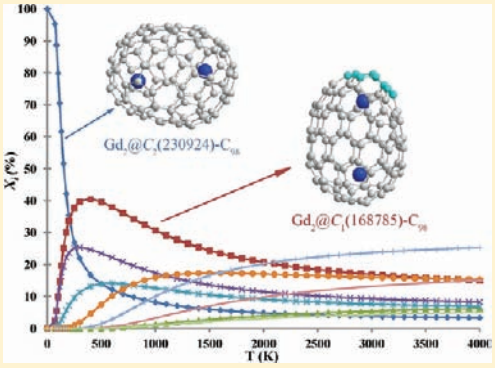

1. INTRODUCTION

Endohedral metallofullerenes (EMFs) have attracted broad interest because of their unique structures, fascinating properties, and potential applications in biomedicine, electronics, photovoltaics, and materials science.[1−5] After lanthanum was first encapsulated inside carbon cages successfully,[6] a large amount of endohedral metallofullerenes have been reported, where the metals mainly from groups II and III[7] and all lanthanides as well as their corresponding metallic nitride clusters,[8] metallic carbides,[9] noble gases,[10] phosphorus,[11] nitrogen,[12] and even metal oxides[13] are encapsulated into various fullerene structures.

To date, lots of large endohedral metallofullerenes have been synthesized and isolated experimentally. In 2000, a series of dysprosium-containing as well as erbium-containing di-EMFs were separated with the cage from C_{80} to C_{94}.[14] In 2006, Yang and Dunsch successfully produced a family of di- and tridysprosium fullerenes from C_{94} to C_{100}, of which electronic properties and optical band gaps were investigated by UV−vis−NIR spectroscopy.[15] Furthermore, Mercado et al. isolated the disamarium fullerene,[16] $Sm_2@C_{104}$-$D_{3d}(822)$, which is the largest endohedral fullerene to be crystallographically characterized to date. Moreover, the complete series of digadolinium endohedral metallofullerenes from $Gd_2@C_{96}$ to $Gd_2@C_{106}$ was obtained recently.[17] Meanwhile, Echegoyen and co-workers also synthesized and isolated several species of trimetallic nitride template endohedral metallofullerenes (TNT EMFs), $M_3N@C_{2n}$ (M = La, Ce, Pr, and Nd; n = 40−55).[18]

Although numerous reports on the synthesis of large EMFs are presented,[14−18] only a few cage structures of these EMFs have been determined[19] to date due to a general difficulty for X-ray structural assignment and ^{13}C NMR spectrum. For C_{98}-based endohedral metallofullerenes, Popov and Dunsch calculated the hexa-anions of the isomers satisfying the isolated pentagon rule (IPR) of C_{98} and predicted the 166:C_2 isomer to be the best candidate for the TNT cluster.[20] Poblet et al. examined the IPR hexa-anions of C_{98} and suggested that the most stable hexa-anions for encapsulation of the M_2 or TNT cluster would be 215:D_3.[21] Nevertheless, in their work, only a part of IPR isomers were taken into account and non-IPR isomers which should be of great importance in some EMFs were neglected. The encapsulated moieties might stabilize the fused pentagons and even enhance the relative stability of metallofullerenes, since the existence of metals or clusters in the cage could reduce the surface tension and make the structure stable. Consequently, the electronic stabilization between the encapsulate moiety and the cage could make some fullerenes of different sizes and symmetries that violate the isolated pentagon rule become available templates for EMFs. Indeed, a lot of

Received: July 24, 2011
Published: January 30, 2012

   dx.doi.org/10.1021/ic201585j | Inorg. Chem. 2012, 51, 2039−2045

EMFs based on non-IPR cages have been synthesized, isolated, and characterized experimentally.[22−29] As a result, non-IPR isomers should also been taken into the theoretical consideration while investigating the structures and properties of EMFs.

In this paper, a comprehensive theoretical calculation has been carried out to discuss the large dimetallofullerenes, $Gd_2@C_{98}$, for the first time. Gadolinium-containing endohedral fullerenes are chosen here since they may contribute to the development of a second generation of relaxation agents for magnetic resonance imaging (MRI).[30] It has been shown on isomeric sets of fullerenes that potential energy itself cannot generally decide stability order at high temperatures as the entropic part of the Gibbs energy becomes essential.[32] Hence, the temperature−entropy effects by the Gibbs free energy function are taken into account in order to obtain deeper insight into the thermodynamic stability of $Gd_2@C_{98}$.

2. COMPUTATIONAL DETAILS

For C_{98} fullerene, there are 231 017 possible cage isomers (227 934 × C_1, 2029 × C_2, 952 × C_s, 27 × C_3, 58 × C_{2v}, 13 × D_3, 1 × C_{3h}, 1 × C_{3v}, 2 × D_{3h}) containing only pentagons and hexagons in their structures, and only 259 isomers of them obey the isolated pentagon rule (IPR).[31,33] In general, those elusive non-IPR fullerenes are regarded to be unstable and impossible of separation in the pristine fullerene form, since adjacent pentagons eventually create quite large ring strain and energy penalty.[34,35] Nevertheless, non-IPR fullerenes could be stabilized[7,22−29] as some kinds of endohedral metallofullerenes because of the strong electronic interaction of the encapsulated metal ions with adjacent pentagon pairs in carbon cages. Considering that the metal atoms are mainly located upon the fused pentagons in the non-IPR endohedral metallofullerenes, the isomers with three or more adjacent pentagon pairs could not be efficiently stabilized by two gadolinium atoms (or dimer) and would be less stable. Thus, it is reasonable to choose all 259 IPR structures and non-IPR species with less than three adjacent pentagons (number of pentagon adjacency denoted by PA, namely, PA = 0−2) as appropriate candidates of metallofullerenes. Therefore, under such a restriction, total 17 941 C_{98} cage isomers have been investigated thoroughly in the present work.

All those 17 941 isomers[31] were primarily screened on the hexa-anion state at the AM1[36] level to evaluate the energetics for the C_{98} isomeric set. Then, the 10 most stable IPR isomers and 5 most stable PA = 1 isomers were further optimized at the hybrid density functional theory B3LYP[37] level with 6-31G(d) basis set. Geometry optimizations of $Gd_2@C_{98}$ based on the most stable C_{98}^{6-} isomers were performed at the B3LYP/3-21G-CEP level with the split-valence 3-21G basis set for carbon and CEP-31G[38] basis set with the corresponding pseudopotential for Gd atoms. All DFT calculations were performed employing the Gaussian 03 program package.[39]

Rotational−vibrational partition functions were constructed from the computed structural and vibrational data at the B3LYP/3-21G-CEP level of theory (though only of the rigid rotator and harmonic oscillator quality and with no frequency scaling). Relative concentrations (mole fractions) w_i of m isomers can be expressed through the partition functions q_i and the ground-state energies $\Delta H^{\circ}_{0,i}$ by a compact formula

$$w_i = \frac{q_i \exp[-\Delta H^{\circ}_{0,i}/(RT)]}{\sum_{j=1}^{m} q_i \exp[-\Delta H^{\circ}_{0,j}/(RT)]} \quad (1)$$

where R is the gas constant and T is the absolute temperature. Clearly enough, the conventional heats of formation at room temperature $\Delta H^{\circ}_{f,298}$ have to be converted to the heats of formation at the absolute zero temperature $\Delta H^{\circ}_{f,0}$. Chirality contributions, frequently ignored, must be also considered in eq 1 as its partition function q_i is doubled for an enantiomeric pair. In this way, the equilibrium concentrations can finally be evaluated, where the partial thermodynamic equilibrium is described by a set of equilibrium constants so that both enthalpy and entropy terms are considered accordingly. Note that eq 1 is an exact relationship derived from the principle of equilibrium statistical thermodynamics, that is, from the standard Gibbs energies of isomers, and it is strongly temperature dependent. All entropy contributions are evaluated through the isomeric partition functions.

3. RESULTS AND DISCUSSION

In EMFs, the encapsulated metal atom or cluster donates electrons to the fullerene cage, giving rise to a negatively charged electronic structure of the fullerene cage.[1−5,40] The carbon-cage isomerism of EMFs shows a good correlation with the relative stabilities of appropriately charged empty cages. Consequently, the screening of a metallofullerene structure usually begins by considering the charged empty cages. Since the electronic structure of $Gd_2@C_{98}$ can be described as $(M^{3+})_2@C_{98}^{6-}$, the C_{98}^{6-} hexa-anions were computed first. On the basis of the extensive AM1 results (see Supporting Information for details), several lowest energy hexa-anions and the corresponding $Gd_2@C_{98}$ were selected and subjected to further geometry optimizations and vibrational analyses all at the B3LYP/3-21G-CEP level of theory. Relative energies and SOMO−LUMO gaps of C_{98}^{6-} and $Gd_2@C_{98}$ are listed in Table 1.

Table 1. Relative Energies and SOMO−LUMO Gaps of C_{98}^{6-} and $Gd_2@C_{98}$ at the B3LYP Level

C_{98}			C_{98}^{6-}		$Gd_2@C_{98}$	
spiral ID	PA	sym	ΔE, kcal/mol	gap, eV	ΔE, kcal/mol	gap, eV
230924	0	C_2	0.00	1.80	0.00	1.35
176408	1	C_1	15.00	1.99	0.41	1.74
168785	1	C_1	11.16	2.20	0.49	1.85
168764	1	C_1	16.89	2.09	0.74	1.93
230933	0	C_1	10.74	1.41	1.97	1.45
230926	0	C_1	11.27	1.37	4.78	1.35
231010	0	C_2	7.42	1.75	6.37	1.05
231005	0	C_1	3.71	1.85	6.77	1.14
230979	0	C_2[a]	11.61	1.29	6.87	1.43
225816	1	C_2[a]	23.82	1.90	12.71	1.13
230927	0	C_1	22.09	1.07	14.97	1.34
230925	0	C_{2v}[b]	12.61	1.23	20.69	0.77
230728	1	C_s	26.68	1.28	26.46	0.93
218092	2	C_1	29.84	2.11	34.28	0.83

[a]The symmetry changes to C_1 after being encapsulated by Gd atoms. [b]The symmetry changes to C_s after encapsulated Gd atoms.

It is revealed that an IPR isomer 230924:C_2[31] is the ground state of C_{98} at the hexa-anion state. The second and third lowest energy structures of hexa-anion C_{98} are also IPR isomers 231005:C_1 and 231010:C_2, respectively. Although it is known that the fused pentagons are unfavorable to the stabilities of carbon cages, several non-IPR isomers with one pentagon pair, such as 168785:C_1, 176408:C_1, and 168764:C_1, are found to possess relatively low energies mainly owing to the strong electronic interaction of the encapsulated metal ions with the pentagon adjacencies. However, relative energies for most isomers with two adjacent pentagons are found to be quite high, indicating the chemical instability.

After encapsulation of two Gd atoms into the cage, the order of relative energies shows some changes compared with that of pristine C_{98} cages at the hexa-anion state. It is demonstrated in

dx.doi.org/10.1021/ic201585j | Inorg. Chem. 2012, 51, 2039−2045

Table 1 that a metallofullerene isomer with IPR structure 230924:C_2, denoted by $Gd_2@C_2(230924)$-C_{98}, is the lowest energy structure with a SOMO−LUMO gap of 1.35 eV at the B3LYP/3-21G-CEP level. The three following stable structures with a relative energy difference less than 1.0 kcal/mol compared to the ground state $Gd_2@C_2(230924)$-C_{98} are discovered to be novel non-IPR isomers wholly with one pair of adjacent pentagons. Notably, the SOMO−LUMO gaps of those non-IPR species are significantly larger than that of $Gd_2@C_2(230924)$-C_{98}, indicating their specific kinetic stabilities. Some other stable IPR isomers at the hexa-anion state display some higher energy after encapsulation of Gd atoms. It is worthy to note that the species with two pairs of pentagon adjacency still behaves with a relatively high energy of 34.28 kcal/mol above the ground state. The energy interchange confirms that the interaction between the encapsulated metals and the cages could stabilize the less stable isomers, especially for the case of non-IPR species, and might vary in terms of different isomers.

For the system of $Gd_2@C_{98}$, because of the small energy differences among the four lowest energy isomers, only the separation energy itself cannot predict relative stabilities in an isomeric system at high temperatures, as stability interchanges induced by the enthalpy−entropy interplay are possible. To obtain a deeper insight into the thermodynamic stability of $Gd_2@C_{98}$, we investigated the entropy effects and evaluated the relative concentrations through the Gibbs free energy terms. Here, we only select and focus on the structures with separation energy below some 30 kJ/mol in the $Gd_2@C_{98}$ equilibrium isomeric mixture, and so only nine lower energy isomers are counted for equilibrium statistical thermodynamic analyses in the present work.

The DFT-based temperature development of relative concentrations of nine $Gd_2@C_{98}$ isomers in a broad temperature region is presented in Figure 1. The $Gd_2@C_2(230924)$-C_{98}, which is the lowest energy structure, must be prevailing at very low temperatures. However, as the temperature increases, its relative concentration declines rapidly and is surpassed by two non-IPR species $Gd_2@C_1(168785)$-C_{98} and $Gd_2@C_1(176408)$-C_{98} around 200 K and finally become very slight beyond 2000 K. Then, at a temperature of 400 K the relative concentration of $Gd_2@C_1(168785)$-C_{98} ascends to its maximum yield of 40.4% compared to the $Gd_2@C_2(230924)$-C_{98} species with a fraction of 16.7%. It is clearly shown that the non-IPR isomer $Gd_2@C_1(168785)$-C_{98} is the most important structure in a broad temperature region from 200 to 2000 K. Moreover, two other non-IPR structures, $Gd_2@C_1(176408)$-C_{98} and $Gd_2@C_1(168764)$-C_{98} also have considerable concentrations before 500 K, though they become less important at higher temperatures. Note that some other IPR isomers $Gd_2@C_1(230926)$-C_{98}, $Gd_2@C_1(230933)$-C_{98}, and $Gd_2@C_2(231010)$-C_{98} perform proper thermodynamic stabilities. The rest of the isomers do not show any distinct stability compared with the $Gd_2@C_1(168785)$-C_{98} species throughout the whole temperature region. It is well known that metallofullerene formation occurs at high temperatures, which is widely regarded between 500 and 3000 K. Even though some isomers exhibit partly comparable relative fractions, the non-IPR structure, $Gd_2@C_1(176408)$-C_{98}, shows the most significant thermodynamic stability in this temperature region. Consequently, the non-IPR $Gd_2@C_1(176408)$-C_{98} species is proposed to be the most probable structure of the $Gd_2@C_{98}$ complex synthesized and isolated in the experiment.

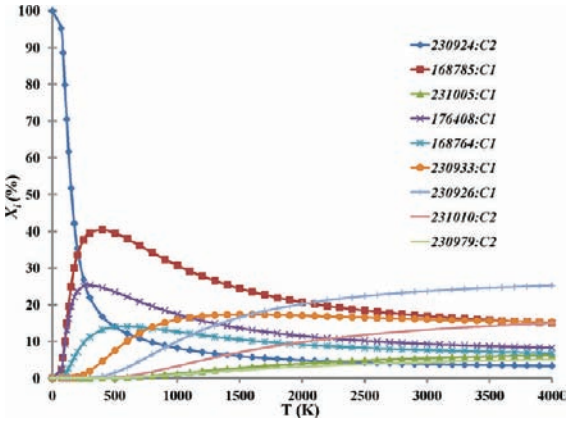

Figure 1. Relative concentrations of the low-energy $Gd_2@C_{98}$ isomers.

Figure 2 shows the top and side views of the optimized structures $Gd_2@C_2(230924)$-C_{98} and $Gd_2@C_1(168785)$-C_{98}. In the case of isomer $Gd_2@C_2(230924)$-C_{98}, two Gd atoms are coordinated to the C_2 axis with a distance of 5.66 Å and the shortest Gd−C distance is predicted to be 2.38 Å. In the optimized geometry of $Gd_2@C_1(168785)$-C_{98}, one Gd atom locates upon the fused pentagons, which is similar to the metal ion position determined in other non-IPR endohedral fullerenes such as $Sc_2@C_{66}$ and $La_2@C_{72}$.[41] The reason for such a phenomenon stems from the strong electrostatic interaction between metal and carbon cage.[42] Another Gd atom in $Gd_2@C_1(168785)$-C_{98} stays upon a hexagon with a Gd−Gd distance of 6.09 Å. To date, the determined cage structures of dimetallofullerenes usually belong to IPR species or some non-IPR isomers possessing two pairs of pentagon adjacency

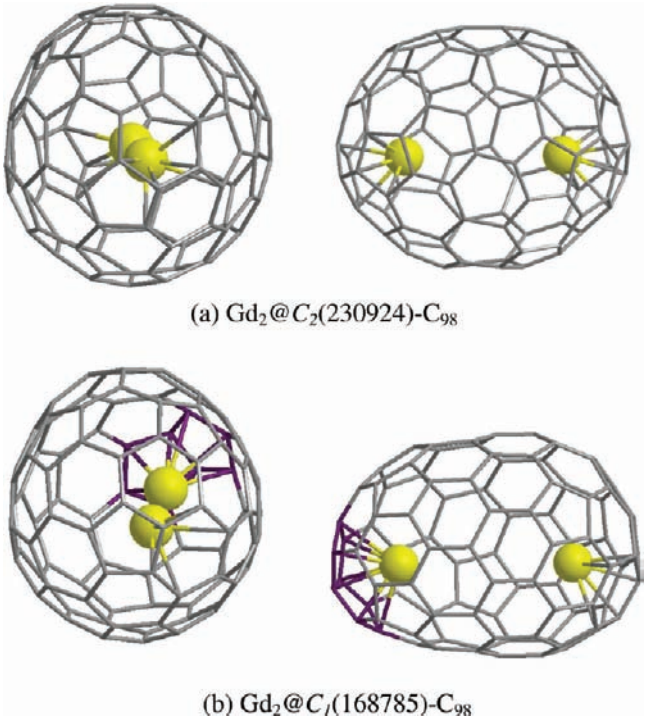

Figure 2. Top (left) and side (right) views of the optimized structures (a) $Gd_2@C_2(230924)$-C_{98} and (b) $Gd_2@C_1(168785)$-C_{98}. Adjacent pentagons are colored violet.

dx.doi.org/10.1021/ic201585j | Inorg. Chem. 2012, 51, 2039−2045

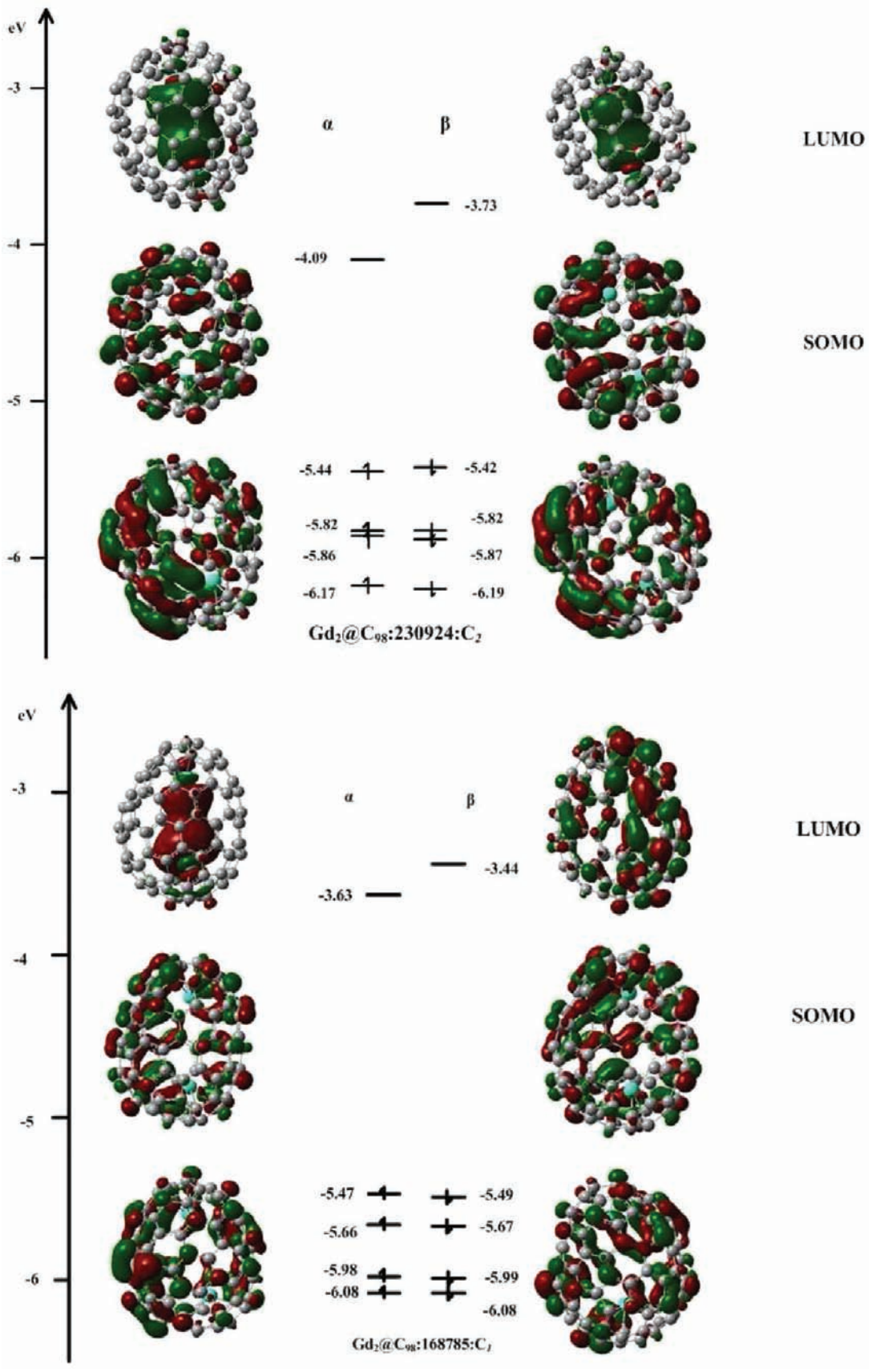

Figure 3. Main frontier molecular orbital diagrams of $Gd_2@C_2(230924)$-C_{98} (top) and $Gd_2@C_1(168785)$-C_{98} (bottom).

such as $Sc_2@C_{66}$ and $La_2@C_{72}$. Interestingly, the novel structure of $Gd_2@C_1(168785)$-C_{98} is ascertained as the first dimetallofullerenes only with one pair of pentagon adjacency, and its shortest Gd−C distance is 2.40 Å.

dx.doi.org/10.1021/ic201585j | Inorg. Chem. 2012, 51, 2039−2045

Figure 3 illustrates the main frontier orbital diagrams of two main metallofullerene isomers $Gd_2@C_2(230924)$-C_{98} and $Gd_2@C_1(168785)$-C_{98}. It is revealed that in both structures the SOMO orbitals are mainly contributed by the carbon cage and the LUMO orbital is chiefly distributed on the metal atoms like the case of other endohedral dimetallofullerenes reported.

Why three new non-IPR metallofullerenes ($Gd_2@C_1(168785)$-C_{98}, $Gd_2@C_1(176408)$-C_{98}, and $Gd_2@C_1(168764)$-C_{98}) are almost isoenergetic in comparison with the lowest energy IPR isomer ($Gd_2@C_2(230924)$-C_{98})? To explore this question, Mulliken charge distributions of $Gd_2@C_{98}$ are needed to be analyzed. Here, we only focus two representative structures, $Gd_2@C_2(230924)$-C_{98} and $Gd_2@C_1(168785)$-C_{98}.

The Mulliken charge distributions of $Gd_2@C_2(230924)$-C_{98} and $Gd_2@C_1(168785)$-C_{98} are depicted in Figure 4. For both

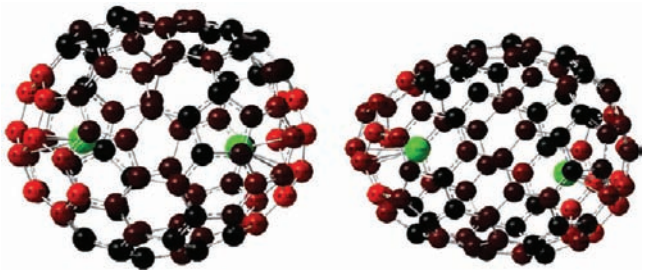

Figure 4. Mulliken charge distributions of $Gd_2@C_2(230924)$-C_{98} (left) and $Gd_2@C_1(168785)$-C_{98} (right). Green represents positive charge, and red represents negative charge.

structures, the carbon cage is negatively charged and the Gd atoms exhibit positive states. Compared with the "equator" of the cages, large positive charges mainly distribute on the poles of cages. In the $Gd_2@C_1(168785)$-C_{98}, the charge of two carbon atoms connecting adjacent pentagons is −0.054 and −0.082, respectively. Interestingly, the number of negatively charged carbon atoms at the adjacent pentagon pole is larger than that at other poles. In other words, the electrons are much more decentralized at the adjacent pentagon pole, resulting in a strong electronic interaction between the positive metal and the fused pentagon with negative charge. Because of this important electrostatic interaction, the non-IPR EMF species could show a high relative stability as $Gd_2@C_1(168785)$-C_{98} does in the present work.

Since theoretical IR spectra may assist the experimental identification of metallofullerenes and provide some valuable information on the distinct cage structures, harmonic vibration frequencies and infrared absorption intensities of the stable $Gd_2@C_{98}$ isomers have been evaluated at the B3LYP/3-21G-CEP level. As shown in Figure 5, there exist two major regions in both spectra: the first one (1000−1700 cm^{-1}) corresponds to a C−C stretching mode and the second one (200−1000 cm^{-1}) corresponds to a cage breathing mode. Obviously, the adsorption intensity is similar for $Gd_2@C_1(168785)$-C_{98} and $Gd_2@C_2(230924)$-C_{98} in the range 200−1000 cm^{-1}. Nevertheless, one apparent difference is exhibited on the vibrational intensity at 1000−1700 cm^{-1} range between $Gd_2@C_1(168785)$-C_{98} and $Gd_2@C_2(230924)$-C_{98}, which is helpful to identify two molecular structures. For example, $Gd_2@C_2(230924)$-C_{98} displays only one intensive peak at 1400 cm^{-1}, while $Gd_2@C_1(168785)$-C_{98} shows several similar peaks with regular intensity in the area of 1340−1400 cm^{-1}. Moreover, one

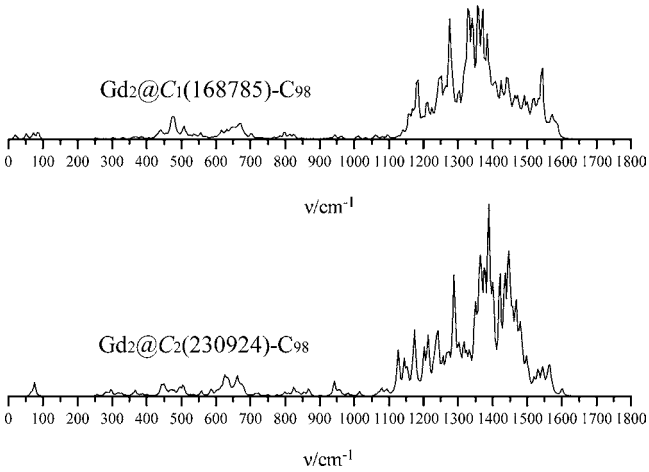

Figure 5. Simulated IR spectra of $Gd_2@C_1(168785)$-C_{98} (top) and $Gd_2@C_2(230924)$-C_{98} (bottom).

distinct sharp absorption peak at 1542 cm^{-1} for structure $Gd_2@C_1(168785)$-C_{98} is presented, in contrast to the lower absorption bands displaying at the same region for $Gd_2@C_2(230924)$-C_{98}.

4. CONCLUSIONS

A systemically theoretical investigation has been performed on the large gadolinium-containing endohedral dimetallofullerene $Gd_2@C_{98}$ by a hybrid density functional theory technique. An IPR isomer, $Gd_2@C_2(230924)$-C_{98}, is predicted as the lowest energy structure followed by three non-IPR isomers on the basis of B3LYP/3-21G-CEP optimizations. Entropy effects have also been investigated to clarify relative stabilities at high temperatures, and statistical equilibrium concentration interchanges evaluated through the Gibbs free energy terms indicate that a novel non-IPR species $Gd_2@C_1(168785)$-C_{98} is the most thermodynamically stable structure within a broad temperature interval related to fullerene formation. Furthermore, the $Gd_2@C_1(168785)$-C_{98} structure also possesses a high kinetic stability due to its larger SOMO−LUMO gap. As a consequence, it is convinced that the newly found non-IPR structure, C_{98}-168785:C_1, should be the most suitable host cage for encapsulation of the Gd_2 group, which is also the largest non-IPR carbon cage for EMFs found so far. The analyses on the Mulliken charge distribution and main molecular orbital diagrams reveal a strong electrostatic interaction between the metal and fused pentagons. In addition, the IR spectra for two isomers are simulated theoretically, which may be helpful to further experimental identification of $Gd_2@C_{98}$. The present work could supply some valuable guidance for the synthesis and experimental characterization of large endohedral metallofullerenes and the corresponding derivatives.

■ ASSOCIATED CONTENT

Supporting Information

The AM1 optimized relative energies of 500 lower energy C98 isomers at hexa-anion state, and Cartesian coordinates of two major Gd2@C98 isomers optimized at the B3LYP level. This material is available free of charge via the Internet at http://pubs.acs.org.

dx.doi.org/10.1021/ic201585j | Inorg. Chem. 2012, 51, 2039−2045

AUTHOR INFORMATION

Corresponding Author

*Phone: +86 29 8266 5671. Fax: +86 29 8266 8559. E-mail: xzhao@mail.xjtu.edu.cn.

ACKNOWLEDGMENTS

This work was partially supported by the National Natural Science Foundation of China (NSFC Grant No. 21171138), the National Key Basic Research Program of China (No. 2012CB720904), the Key Project in the National Science and Technology Pillar Program of China (Grant No. 2010BAK67B12), and the Grand-in-Aid for the Specially Promoted Research from MEXT of Japan. X.Z. is thankful for the special support from the Tengfei Talent Project of Xi'an Jiaotong University. The Ministry of Education (MOE) Key Laboratory for Nonequilibrium Condensed Matter and Quantum Engineering at Xi'an Jiaotong University and the Research Center for Basic Science (XJTU) are also appreciated.

REFERENCES

(1) Shinohara, H. *Rep. Prog. Phys.* **2000**, *63*, 843−892.

(2) Akasaka, T.; Nagase, S. *Endofullerenes: A New Family of Carbon Clusters*; Kluwer: Dordrecht, 3 2002.

(3) Chaur, M. N.; Melin, F.; Ortiz, A. L.; Echegoyen, L. *Angew. Chem., Int. Ed.* **2009**, *48*, 7514−7538.

(4) Akasaka, T.; Wudl, F.; Nagase, S. *Chemistry of Nanocarbons*; Wiley-Blackwell: London, 2010.

(5) Lu, X.; Akasaka, T.; Nagase, S. *Chem. Commun.* **2011**, *47*, 5942−5957.

(6) Chai, Y.; Guo, T.; Jin, C. M.; Haufler, R. E.; Chibante, L. P. F; Fure, J.; Wang, L. H.; Alford, J. M.; Smalley, R. E. *J. Phys. Chem.* **1991**, *95*, 7564−7568.

(7) (a) Wang, C. R.; Kai, T.; Tomiyama, T.; Yoshida, T.; Kobayashi, Y.; Nishibori, E.; Takata, M.; Sakata, M.; Shinohara, H. *Nature* **2001**, *408*, 426−427. (b) Takata, M.; Nishibori, E.; Sakata, M.; Wang, C. R.; Shinohara, H. *Chem. Phys. Lett.* **2003**, *372*, 512−518. (c) Kato, H.; Taninaka, A.; Sugai, T.; Shinohara, H. *J. Am. Chem. Soc.* **2003**, *125*, 7782−7783. (d) Cao, B. P.; Hasegawa, M.; Okada, K.; Tomiyama, T.; Okazaki, T.; Suenaga, K.; Shinohara, H. *J. Am. Chem. Soc.* **2001**, *123*, 9679−9680. (e) Iwasaki, K.; Hino, S.; Yoshimura, D.; Cao, B. P.; Okazaki, T.; Shinohara, H. *Chem. Phys. Lett.* **2004**, *397*, 169−173. (f) Liu, S.; Sun, S. *J. Organomet. Chem.* **2000**, *599*, 74−86.

(8) (a) Dunsch, L.; Yang, S. *Phys. Chem. Chem. Phys.* **2007**, *9*, 3067−3081. (b) Dunsch, L.; Yang, S. *Small* **2007**, *3*, 1298−1320.

(9) Wang, C.-R.; Kai, T.; Tomiyama, T.; Yoshida, T.; Kobayashi, Y.; Nishibori, E.; Takata, M.; Sakata, M.; Shinohara, H. *Angew. Chem., Int. Ed.* **2001**, *40*, 397−399.

(10) (a) Saunders, M.; Jimenez-Vazquez, H. A.; Cross, R. J.; Mroczkowski, M.; Gross, M. L.; Giblin, D. E.; Poreda, R. J. *J. Am. Chem. Soc.* **1994**, *116*, 2193−2194. (b) Syamala, M. S.; Cross, R. J.; Saunders, M. *J. Am. Chem. Soc.* **2002**, *124*, 6216−6219.

(11) Larsson, J. A.; Greer, J. C.; Harneit, W.; Weidinger, A. *J. Chem. Phys.* **2002**, *116*, 7849−7854.

(12) Mauser, H.; Hirsch, A.; van Eikema Hommes, N. J. R.; Clark, T.; Pietzak, B.; Weidinger, A.; Dunsch, L. *Angew. Chem., Int. Ed. Engl.* **1997**, *36*, 2835−2838.

(13) Stevenson, S.; Mackey, M. A.; Stuart, M. A.; Phillips, J. P.; Easterling, M. L.; Chancellor, C. J.; Olmstead, M. M.; Balch, A. L. *J. Am. Chem. Soc.* **2008**, *130*, 11844−11845.

(14) (a) Tagmatarchis, N.; Shinohara, H. *Chem. Mater.* **2000**, *12*, 3222−3226. (b) Tagmatarchis, N.; Aslanis, E.; Prassides, K.; Shinohara, H. *Chem. Mater.* **2001**, *13*, 2374−2379.

(15) Yang, S.; Dunsch, L. *Angew. Chem., Int. Ed.* **2006**, *45*, 1299−1302.

(16) Mercado, B. Q.; Jiang, A.; Yang, H.; Wang, Z.; Jin, H.; Liu, Z.; Olmstead, M. M.; Balch, A. L. *Angew. Chem., Int. Ed.* **2009**, *48*, 9114−9116.

(17) Yang, H.; Lu, C.; Liu, Z.; Jin, H.; Che, Y.; Olmstead, M. M.; Balch, A. L. *J. Am. Chem. Soc.* **2008**, *130*, 17296−17300.

(18) (a) Chaur, M. N.; Melin, F.; Elliott, B.; Kumbhar, A.; Athans, A. J.; Echegoyen, L. *Chem.—Eur. J.* **2008**, *14*, 4594−4599. (b) Chaur, M. N.; Melin, F.; Ashby, J.; Elliott, B.; Kumbhar, A.; Rao, A. M.; Echegoyen, L. *Chem.—Eur. J.* **2008**, *14*, 8213−8219.

(19) (a) Valencia, R.; Rodíguez-Fortea, A.; Clotet, A.; de Graaf, C.; Chaur, M. N.; Echegoyen, L.; Poblet, J. M. *Chem.—Eur. J.* **2009**, *15*, 10997−11009. (b) Yang, T.; Zhao, X.; Nagase, S. *Phys. Chem. Chem. Phys.* **2011**, *13*, 5034−5037.

(20) Valencia, R.; Rodíguez-Fortea, A.; Poblet, J. M. *Chem.Commun.* **2007**, 4161−4163.

(21) Popov, A. A.; Dunsch, L. *J. Am. Chem. Soc.* **2007**, *129*, 11835−11849.

(22) Kobayashi, K.; Nagase, S.; Yoshida, M.; Ōsawa, E. *J. Am. Chem. Soc.* **1997**, *119*, 12693−12694.

(23) Stevenson, S.; Fowler, P. W.; Heine, T.; Duchamp, J. C.; Rice, G.; Glass, T.; Harich, K.; Hajdu, E.; Bible, R.; Dorn, H. C. *Nature* **2000**, *408*, 427−428.

(24) Wakahara, T.; Nikawa, H.; Kikuchi, T.; Nakahodo, T.; Rahman, G. M. A.; Tsuchiya, T.; Maeda, Y.; Akasaka, T.; Yoza, K.; Horn, E.; Yamamoto, K.; Mizorogi, N.; Slanina, Z.; Nagase, S. *J. Am. Chem. Soc.* **2006**, *128*, 14228−14229.

(25) Zuo, T.; Walker, K.; Olmstead, M. M.; Melin, F.; Holloway, B. C.; Echegoyen, L.; Dorn, H. C.; Chaur, M. N.; Chancellor, C. J.; Beavers, C. M.; Balch, A. L.; Athans, A. J. *Chem. Commun.* **2008**, 1067−1069.

(26) Lu, X.; Nikawa, H.; Tsuchiya, T.; Maeda, Y.; Ishitsuka, M. O.; Akasaka, T.; Toki, M.; Sawa, H.; Slanina, Z.; Mizorogi, N.; Nagase, S. *Angew. Chem., Int. Ed.* **2008**, *47*, 8642−8645.

(27) Lu, X.; Nikawa, H.; Nakahodo, T.; Tsuchiya, T.; Ishitsuka, M. O.; Maeda, Y.; Akasaka, T.; Toki, M.; Sawa, H.; Slanina, Z.; Mizorogi, N.; Nagase, S. *J. Am. Chem. Soc.* **2008**, *130*, 9129−9136.

(28) Beavers, C. M.; Chaur, M. N.; Olmstead, M. M.; Echegoyen, L.; Balch, A. L. *J. Am. Chem. Soc.* **2009**, *131*, 11519−11524.

(29) Yang, T.; Zhao, X.; Xu, Q.; Zhou, C. H.; He, L.; Nagase, S. *J. Mater. Chem.* **2011**, *21*, 12206−12209.

(30) Caravan, P.; Ellison, J. J.; McMurry, T. J.; Lauffer, R. B. *Chem. Rev.* **1999**, *99*, 2293−2352.

(31) (a) Fowler, P. W.; Manoloupoulos, D. E. *An Atlas of Fullerenes*; Oxford University Press: Oxford, 1995. (b) Zhao, X. *J. Phys. Chem. B* **2005**, *109*, 5267−5272.

(32) Slanina, Z.; Uhĺík, F.; Zhao, X.; Ōsawa, E. *J. Chem. Phys.* **2000**, *113*, 4933−4937.

(33) Zhao, X.; Slanina, Z. *J. Mol. Struct. (THEOCHEM)* **2003**, *636*, 195−201.

(34) Albertazzi, E.; Domene, C.; Fowler, P. W.; Heine, T.; Seifert, G.; Van Alsenoy, C.; Zerbetto, F. *Phys. Chem. Chem. Phys.* **1999**, *1*, 2913−2918.

(35) Campbell, E. E. B.; Fowler, P. W.; Mitchell, D.; Zerbetto, F. *Chem. Phys. Lett.* **1996**, *250*, 544−548.

(36) Dewar, M. J. S.; Zoebisch, E.; Healy, E. F.; Stewart, J. J. P. *J. Am. Chem. Soc.* **1985**, *107*, 3902−3909.

(37) (a) Becke, A. D. *Phys. Rev. A* **1988**, *38*, 3098−3100. (b) Becke, A. D. *J. Chem. Phys.* **1993**, *98*, 5648−5652. (c) Lee, C.; Yang, W.; Parr, R. G. *Phys. Rev. B: Condens. Matter Mater. Phys.* **1988**, *37*, 785−789.

(38) Cundari, T. R; Stevens, W. J. *J. Chem. Phys.* **1993**, *98*, 5555−5565.

(39) Frisch, M. J.; Trucks, G. W.; Schlegel, H. B.; Scuseria, G. E.; Robb, M. A.; Cheeseman, J. R.; Montgomery, J. A.; Vreven, J. T.; Kudin, K. N.; Burant, J. C.; Millam, J. M.; Iyengar, S. S.; Tomasi, J.; Barone, V.; Mennucci, B.; Cossi, M.; Scalmani, G.; Rega, N.; Petersson, G. A.; Nakatsuji, H.; Hada, M.; Ehara, M.; Toyota, K.; Fukuda, R.; Hasegawa, J.; Ishida, M.; Nakajima, T.; Honda, Y.; Kitao, O.; Nakai, H.; Klene, M.; Li, X.; Knox, J. E.; Hratchian, H. P.; Cross, J. B.; Bakken, V.; Adamo, C.; Jaramillo, J.; Gomperts, R.; Stratmann, R.

E.; Yazyev, O.; Austin, A. J.; Cammi, R.; Pomelli, C.; Ochterski, J. W.; Ayala, P. Y.; Morokuma, K.; Voth, G. A.; Salvador, P.; Dannenberg, J. J.; Zakrzewski, V. G.; Dapprich, S.; Daniels, A. D.; Strain, M. C.; Farkas, O.; Malick, D. K.; Rabuck, A. D.; Raghavachari, K.; Foresman, J. B.; Ortiz, J. V.; Cui, Q.; Baboul, A. G.; Clifford, S.; Cioslowski, J.; Stefanov, B. B.; Liu, G.; Liashenko, A.; Piskorz, P.; Komaromi, I.; Martin, R. L.; Fox, D. J.; Keith, T.; Al-Laham, M. A., Peng, C. Y.; Nanayakkara, A.; Challacombe, M.; Gill, P. M. W.; Johnson, B.; Chen, W.; Wong, M. W.; Gonzalez, C.; Pople, J. A. *Gaussian 03* (Revision E.01); Gaussian, Inc.: Wallingford, CT, 2004.

(40) Yang, T.; Zhao, X.; Osawa, E. *Chem.—Eur. J.* **2011**, *17*, 10230–10234.

(41) (a) Wang, C. R.; Kai, T.; Tomiyama, T.; Yoshida, T.; Kobayashi, Y.; Nishibori, E.; Takata, M.; Sakata, M.; Shinohara, H. *Nature* **2000**, *408*, 426–427. (b) Kato, H.; Taninaka, A.; Sugai, T.; Shinohara, H. *J. Am. Chem. Soc.* **2003**, *125*, 7782–7783. (c) Lu, X.; Nikawa, H.; Nakahodo, T.; Tsuchiya, T.; Ishitsuka, M. O.; Maeda, Y.; Akasaka, T.; Toki, M.; Sawa, H.; Slanina, Z.; Mizorogi, N.; Nagase, S. *J. Am. Chem. Soc.* **2008**, *130*, 9129–9136. (d) Lu, X.; Nikawa, H.; Tsuchiya, T.; Maeda, Y.; Ishitsuka, M. O.; Akasaka, T.; Toki, M.; Sawa, H.; Slanina, Z.; Mizorogi, N.; Nagase, S. *Angew. Chem., Int. Ed.* **2008**, *47*, 8642–8645.

(42) Martín, N. *Angew. Chem., Int. Ed.* **2011**, *50*, 5431–5433.